

RESEARCH

Open Access



Identification and transcriptomic assessment of latent profile pediatric septic shock phenotypes

Mihir R. Atreya^{1,2*}, Min Huang³, Andrew R. Moore⁴, Hong Zheng^{4,5}, Yehudit Hasin-Brumshtein⁶, Julie C. Fitzgerald⁷, Scott L. Weiss⁸, Natalie Z. Cvijanovich⁹, Michael T. Bigham¹⁰, Parag N. Jain¹¹, Adam J. Schwarz¹², Riad Lutfi¹³, Jeffrey Nowak¹⁴, Neal J. Thomas¹⁵, Michael Quasney¹⁶, Mary K. Dahmer¹⁶, Torrey Baines¹⁷, Bereketab Haileselassie¹⁸, Andrew J. Lautz^{1,2}, Natalja L. Stanski^{1,2}, Stephen W. Standage^{1,2}, Jennifer M. Kaplan^{1,2}, Basilia Zingarelli^{1,2}, Rashmi Sahay¹⁹, Bin Zhang¹⁹, Timothy E. Sweeney⁶, Purvesh Khatri^{4,5}, L. Nelson Sanchez-Pinto^{20,21} and Rishikesan Kamaleswaran^{22,23}

Abstract

Background Sepsis poses a grave threat, especially among children, but treatments are limited owing to heterogeneity among patients. We sought to test the clinical and biological relevance of pediatric septic shock subclasses identified using reproducible approaches.

Methods We performed latent profile analyses using clinical, laboratory, and biomarker data from a prospective multi-center pediatric septic shock observational cohort to derive phenotypes and trained a support vector machine model to assign phenotypes in an internal validation set. We established the clinical relevance of phenotypes and tested for their interaction with common sepsis treatments on patient outcomes. We conducted transcriptomic analyses to delineate phenotype-specific biology and inferred underlying cell subpopulations. Finally, we compared whether latent profile phenotypes overlapped with established gene-expression endotypes and compared survival among patients based on an integrated subclassification scheme.

Results Among 1071 pediatric septic shock patients requiring vasoactive support on day 1 included, we identified two phenotypes which we designated as *Phenotype 1* (19.5%) and *Phenotype 2* (80.5%). Membership in *Phenotype 1* was associated with ~fourfold adjusted odds of complicated course relative to *Phenotype 2*. Patients belonging to *Phenotype 1* were characterized by relatively higher Angiotensin-2/Tie-2 ratio, Angiotensin-2, soluble thrombomodulin (sTM), interleukin 8 (IL-8), and intercellular adhesion molecule 1 (ICAM-1) and lower Tie-2 and Angiotensin-1 concentrations compared to *Phenotype 2*. We did not identify significant interactions between phenotypes, common treatments, and clinical outcomes. Transcriptomic analysis revealed overexpression of genes implicated in the innate immune response and driven primarily by developing neutrophils among patients designated as *Phenotype 1*. There was no statistically significant overlap between established gene-expression endotypes, reflective of the host adaptive response, and the newly derived phenotypes, reflective of the host innate response including microvascular endothelial dysfunction. However, an integrated subclassification scheme demonstrated varying survival probabilities when comparing patient endophenotypes.

*Correspondence:

Mihir R. Atreya

Mihir.Atreya@cchmc.org

Full list of author information is available at the end of the article



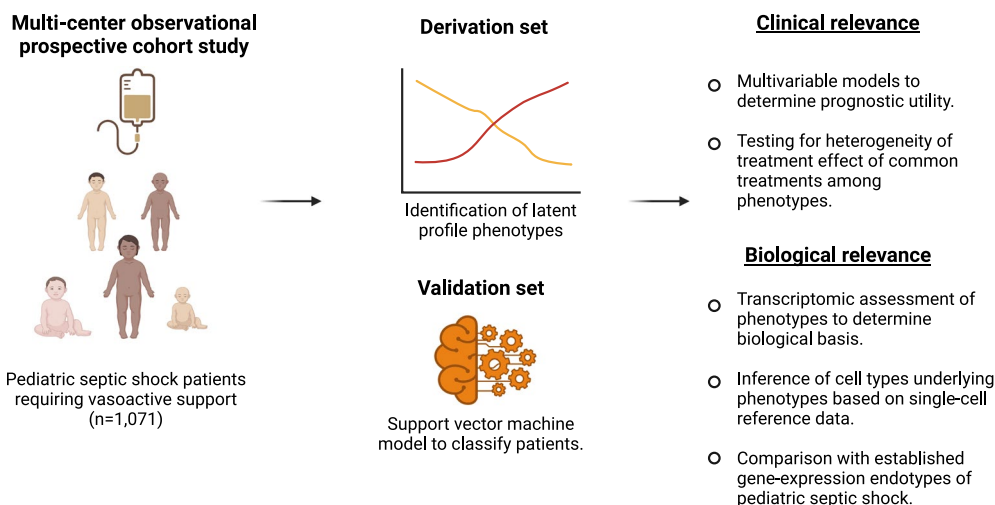
© The Author(s) 2024. **Open Access** This article is licensed under a Creative Commons Attribution 4.0 International License, which permits use, sharing, adaptation, distribution and reproduction in any medium or format, as long as you give appropriate credit to the original author(s) and the source, provide a link to the Creative Commons licence, and indicate if changes were made. The images or other third party material in this article are included in the article's Creative Commons licence, unless indicated otherwise in a credit line to the material. If material is not included in the article's Creative Commons licence and your intended use is not permitted by statutory regulation or exceeds the permitted use, you will need to obtain permission directly from the copyright holder. To view a copy of this licence, visit <http://creativecommons.org/licenses/by/4.0/>. The Creative Commons Public Domain Dedication waiver (<http://creativecommons.org/publicdomain/zero/1.0/>) applies to the data made available in this article, unless otherwise stated in a credit line to the data.

Conclusions Our research underscores the reproducibility of latent profile analyses to identify pediatric septic shock phenotypes with high prognostic relevance. Pending validation, an integrated subclassification scheme, reflective of the different facets of the host response, holds promise to inform targeted intervention among those critically ill.

Keywords Sepsis, Precision medicine, Endotype, Phenotype

Graphical abstract

Identification and transcriptomic assessment of latent profile pediatric septic shock phenotypes.



Atreya et al, *Critical Care*, 2024

Introduction

Sepsis is defined as life-threatening organ dysfunction caused by a dysregulated host response to an infection. It represents a major public health problem, especially among children, where it affects an estimated 20 million each year worldwide [1] and is the leading cause of under-5 mortality [2]. Yet, despite numerous trials, sepsis care remains limited to early antibiotics and intensive organ support. This lack of therapeutic efficacy has been attributed to the heterogeneity among critically ill patients [3]. Thus, reproducible strategies that identify clinically and biologically relevant subclasses are necessary to facilitate targeted approaches to improve patient outcomes [4].

Gene-expression profiling of whole blood has been used to identify sepsis subclasses [5–9]. Among children, Wong and colleagues used a 100 gene-expression panel, to identify pediatric septic shock *Endotypes—A* and *B* with prognostic value; assignment to *Endotype A* was associated with a nearly threefold increased risk of mortality, relative to those with *Endotype B* [10]. Subsequently, these endotypes were shown to demonstrate a

differential response to corticosteroids in observational studies, with patients classified as *Endotype A* having a fourfold increase in mortality with use of adjunctive corticosteroid use, relative to patients with *Endotype B* [11]. Similar strategies have been deployed among adults yielding analogous results [12].

Concomitantly, a decade ago, Calfee et al. leveraged latent class analyses of clinical, laboratory, and biomarker data to identify two phenotypes of acute respiratory distress syndrome (ARDS). The *hyperinflammatory* group was characterized by worse outcomes, relative to those without this phenotype [13]. Of note, these phenotypes have demonstrated heterogeneity in treatment effect (HTE) in response to several interventions in secondary analyses of ARDS trials [13, 14], and corticosteroids among critically ill COVID-19 patients [15]. More recently, Dahmer et al. and others have shown reproducibility and prognostic utility of this approach among children with ARDS [16, 17]. Lastly, using similar approaches, Sinha et al. recently published on molecular phenotypes among adults with sepsis [18]. To the best of our knowledge, no study to

date has identified latent profile phenotypes, inclusive of biomarker data, among critically ill children with sepsis.

In the current study, we sought to derive and internally validate pediatric septic shock phenotypes using latent profile analyses in our multi-center prospective observational cohort and to establish their prognostic value. We sought to test interactions between phenotypes and common treatments on patient outcomes. To establish their biological significance, we conducted transcriptomic analyses in a subset of the cohort to identify differentially expressed genes and infer cell subpopulations linked to phenotypes. Lastly, we compared the overlap between previously established gene-expression endotypes of pediatric septic shock and newly identified latent profile phenotypes. We tested the hypothesis that integrating endotype and phenotype assignment could provide a refined framework for the subclassification of critically ill children.

Methods

Study design and patient selection

Our ongoing prospective observational cohort study of pediatric septic shock has been extensively detailed previously [11, 19–21]. All study procedures involving human participants were per the ethical standards of the institutional review boards of participating institutions and consistent with the 1964 Helsinki Declaration and its later amendments or comparable ethical standards. Briefly, children ≤ 18 years of age were enrolled after informed consent was obtained from parents or legal guardians. Inclusion criteria for study enrollment were all patients meeting consensus criteria for pediatric septic shock [22] recruited between 2003 and 2023 from 13 pediatric intensive care units (PICUs) in the U.S. Blood was collected from consenting participants within 24 h of meeting enrollment criteria (day 1). Patients who did not require any vasoactive support were excluded from the current analyses. The primary outcome of interest was complicated course—a composite endpoint of death by or presence of ≥ 2 organ dysfunctions on day 7 after study enrollment [20]. Secondary outcomes included 7- and 28-day mortality.

Data imputation

We excluded variables with $\geq 40\%$ missingness of data. Among those with $< 40\%$ missingness, we used python package “Datawig” which uses deep learning feature extraction with automatic hyperparameter tuning to impute missing value [23]. Additional methodological details are presented in the Online Supplement.

Derivation set

We randomly split patients in the cohort into derivation (60%) and hold-out internal validation (40%) sets. We used R package “mclust” (v.6.0.0) to perform latent profile analyses (LPA)—a Gaussian Finite Mixture Modeling approach—using clinical, laboratory, and biomarker variables collected on day 1 of septic shock. Briefly, we included deviation of vital signs from the median values for age and sex during health. Laboratory data were obtained at the discretion of treating physicians. The most extreme value for the day were included for these variables. Biomarker data were previously measured using multiplex Luminex assays in serum collected on day 1 [20, 24]. Additional methodological details are presented in the Online Supplement.

Validation set

The phenotype assignments in the derivation set were used to train a support vector machine (SVM) classifier, which was used to assign phenotypes in the validation set using the same set of variables used in the LPA model. We compared patient demographics, characteristics, outcomes in the derivation and validation sets to determine clinical relevance of assigned phenotypes. In sensitivity analyses, we compared biomarkers among identified phenotypes in the validation dataset after exclusion of imputed data to ensure validity and biological relevance of phenotypes.

Transcriptomic analyses

Bulk messenger RNA sequencing data was available from a subset of the cohort recruited between 2019 and 2023 from day 1 biospecimens. We used DESeq2 (v.1.38.3) to identify differentially expressed genes (DEGs) between the latent profile phenotypes. DEGs were selected based on $\geq \log_2$ fold change value cutoff of ± 0.25 , and adjusted p value of 0.05. We conducted Reactome pathway analyses [25] using “ReactomePA” package with a Benjamin Hochberg false discovery rate (FDR) < 0.05 to identify enriched biological pathways.

Inference of cell types underlying phenotypes

We sought to gain granular insight at a single-cell level into immune cell subpopulations associated with latent profile phenotypes. To achieve this, we used a publicly available single-cell RNA sequencing dataset comprised of critically ill adults with sepsis published by Kwok et al. [26] We calculated a composite gene score as the geometric mean of overexpressed genes minus the geometric mean of under-expressed genes using published methods [27], identified through DEG analyses comparing latent profile phenotypes and available in the single-cell dataset.

We mapped the scaled composite score against the Uniform Manifold Approximation and Projection (UMAP) of the single-cell dataset to infer cell types driving biological differences between phenotypes.

Comparison with established gene-expression pediatric septic shock endotypes

A subset of patients in the cohort had existing assignments as *Endotypes A* or *B* based on historical data using a 100-gene panel on the Nanostring nCounter platform. Briefly, image analysis of gene-expression mosaics were previously used to assign pediatric septic shock endotypes, with *Endotype A* being characterized by a repressed adaptive immune response and glucocorticoid signaling, relative to *Endotype B* [11].

Statistical analyses

Minitab (PA, USA) and R were used for statistical analyses. GraphPad (CA, USA) and R were used to generate figures. We assessed differences in demographic and clinical characteristics between groups by non-parametric Kruskal–Wallis tests for continuous variables and χ^2 tests for categorical variables. Multivariable logistic regression models were used to assess the association between phenotype and outcomes of interest and adjusted for era of enrollment (2013–2023 vs. 2003–2012), patient age, pediatric risk of mortality score (PRISM III) [28], presence of comorbidity, and immunocompromised status. We used inverse probability treatment weighting (IPTW) to test the effect of common sepsis treatments on the odds of complicated course among latent profile phenotypes accounting for the effect of multiple confounding variables [29]. Treatments tested included use of > 100 ml/kg versus < 100 ml/kg fluid resuscitation, ≥ 2 versus < 2 antimicrobials, ≥ 2 versus < 2 vasoactive medications on day 1, and corticosteroid use. For IPTW models, we adjusted for age, PRISM-III score, day 1 vasoactive inotropic score (VIS), presence of comorbidity and immunocompromised status. Interaction p values for overall effect were used to test for heterogeneity of treatment effect (HTE) across latent profile phenotypes on complicated course. The Pearson χ^2 test was used to test the overlap between established gene-expression endotypes and latent profile phenotypes. Kaplan Meier curves were used to estimate differences in survival comparing endotypes, phenotypes, and an integrated subclass assignment scheme where we considered outputs of both these approaches. Cox proportional hazard ratio of 28-day mortality among subclasses was compared in reference to the endophenotype with the lowest 28-day mortality. A two-tailed p value < 0.05 was used to test statistical significance, unless otherwise specified.

Results

The overview of the study and analyses is detailed in Fig. 1. A total of 1,395 patients met the inclusion criteria for the study of whom we excluded 324 patients who did not receive any vasoactive support. The median age of the patients included in the study ($n = 1071$) was 5.3 years (quartile 1: 1.7; quartile 3: 11.0 years). The derivation set was comprised of 646 patients and the hold-out validation set included 425 patients. Latent profile analyses in the derivation set revealed two phenotypes. Differences in standardized variables between the two phenotypes are shown in Fig. 2. One of the phenotypes ($n = 126$, 19.5%) was characterized by a relatively higher lactate, serum creatinine, blood urea nitrogen (BUN), and international normalized ratio (INR), and lower platelet

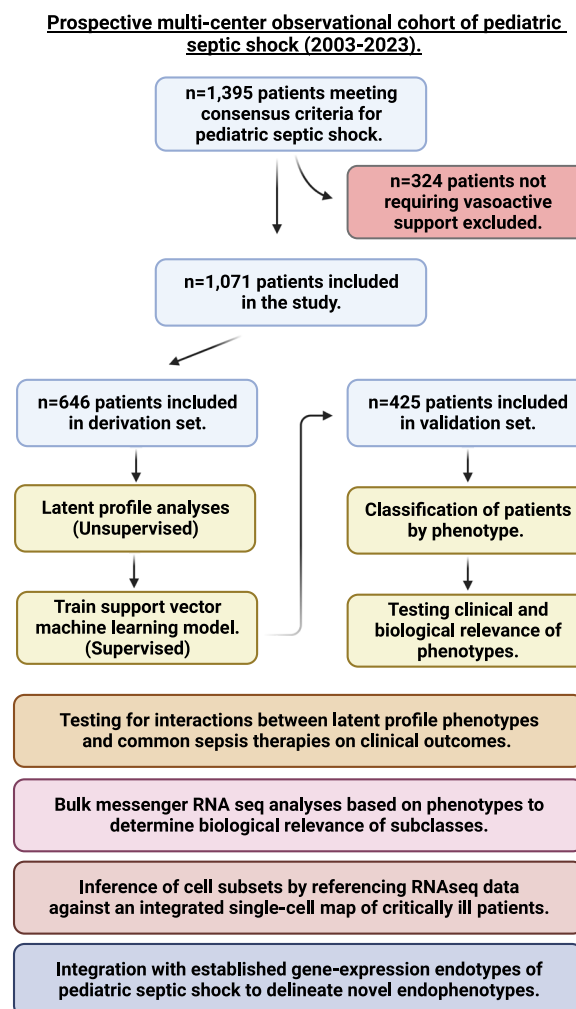


Fig. 1 Overview of study including inclusion and exclusion criteria, number of patients across the derivation and validation set, and various analytic approaches used to characterize latent profile phenotypes of pediatric septic shock

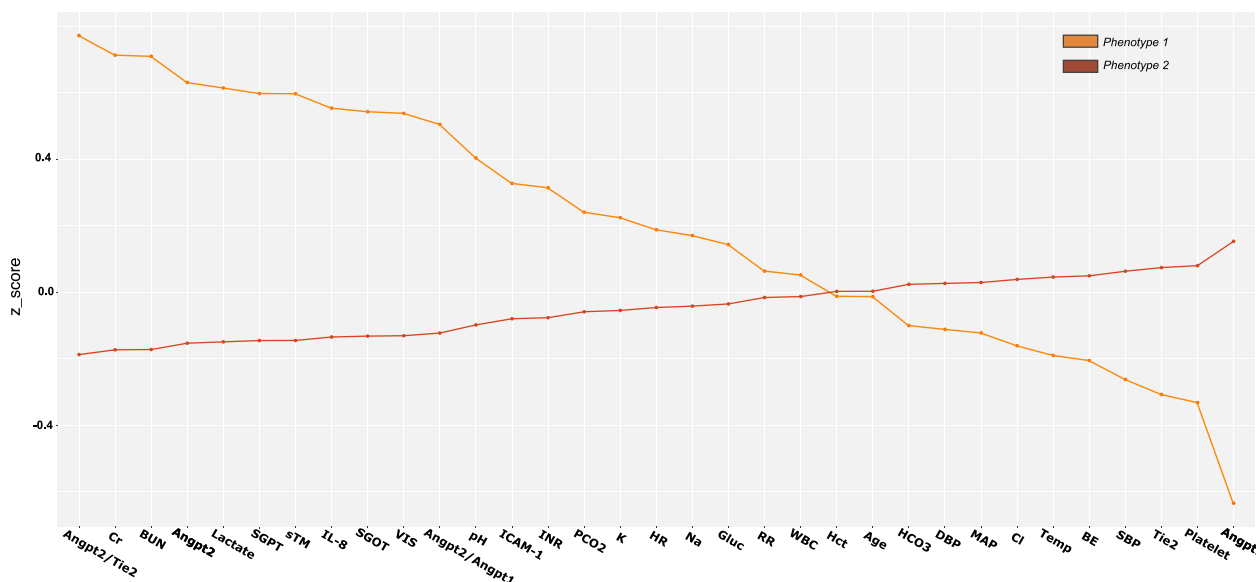


Fig. 2 Standardized mean (z-scores) for continuous class predicting variables in the derivation set by latent profile is shown on the y-axis. The predictor variables are sorted on the x-axis from left to right in descending order of difference between the *Phenotype 1* (shown in orange) and *Phenotype 2* (shown in brown) phenotypes. Angpt2/Tie-2: Angiotensin-2/Tie-2 ratio; Cr: Creatinine; BUN: blood urea nitrogen; Angpt-2: Angiotensin-2; Lactate: Serum lactate; SGPT: serum glutamic pyruvic transaminase; sTM: soluble Thrombomodulin; IL-8: Interleukin-8; SGOT: serum glutamic-oxaloacetic transaminase; VIS: Max vasoactive inotropic score on day 1; Angpt-2/Angpt-1: Angiotensin-2/Angiotensin-1 ratio; pH; ICAM-1: Intercellular adhesion molecule 1; INR: international normalized ratio; PCO2: partial pressure of carbon dioxide; K: potassium; HR: deviation from age and sex normalized heart rate; Na: Sodium; Gluc: Glucose; RR: respiratory rate; WBC: white blood cell count; Hct: hematocrit; Age: age in years; HCO3: serum bicarbonate; DBP: diastolic blood pressure; MAP: mean arterial pressure; Cl: serum chloride; Temp: Temperature; BE: base excess; SBP: systolic blood pressure; Tie-2: tyrosine kinase with immunoglobulin-like loops and epidermal growth factor homology domains-2; Platelet: platelet count; Angpt-1: Angiotensin-1

counts, which we designated as *Phenotype 1*. Patients in this group had relatively higher Angiotensin-2/Tie-2 ratio, Angiotensin-2, soluble thrombomodulin (sTM), interleukin 8 (IL-8), and intercellular adhesion molecule 1 (ICAM-1) and lower Tie-2 and Angiotensin-1 concentrations. We labeled the remaining patients (n=520, 80.5%), characterized by the absence of such features, as *Phenotype 2*.

Table 1 shows the comparisons between phenotypes in the derivation and validation sets—the latter based on the assignments of our SVM classifier. There were no differences in age and sex comparing phenotypes. Although patients who were *Phenotype 1* were more likely to have had a history of oncologic disease or bone marrow transplantation than *Phenotype 2* in the derivation set, there were no statistically significant differences in the validation set. Patients with *Phenotype 1* had a trend toward higher rates of positive blood cultures compared to patients with *Phenotype 2* in the derivation set (26.2% vs. 19.2%, $p=0.08$); this reached statistical significance in the validation set (33.8% vs. 20.6%, $p=0.016$). However, there were no significant differences in the type of pathogen based on culture. Patients with *Phenotype 1* had higher baseline illness severity and significantly worse clinical

outcomes in the derivation and validation sets. Finally, patients with *Phenotype 1* were more likely to have been prescribed corticosteroids by treating physicians, relative to those in *Phenotype 2*.

Table 2 shows the results of multi-variable logistic regression testing the association between latent profile phenotypes and outcomes. Patients belonging to *Phenotype 1* had a nearly fourfold higher odds of complicated course (adj. OR 3.9, 95% CI 2.8–5.5, $p<0.001$) relative to *Phenotype 2*. In addition, these patients had an over fivefold higher odds of 7-day mortality (adj. OR 5.6, 95% CI 3.6–8.6, $p<0.001$) and over fourfold higher odds of 28-day mortality (adj. OR 4.4, 95% CI 3.0–6.4, $p<0.001$). Table 3 shows the results of unadjusted, IPTW adjusted associations, and overall interaction between latent profile phenotypes and common sepsis therapies on odds of complicated course. Patients with *Phenotype 1* were more likely to have received ≥ 100 ml/kg of fluid on day 1 of PICU admission, ≥ 2 antimicrobials, ≥ 2 vasoactive agents, and corticosteroids, with commensurately worse outcomes, relative to those belonging to *Phenotype 2*. We did not identify any significant heterogeneity of treatment effect on outcomes with one exception. Patients belonging to *Phenotype 1* who received ≥ 2 antimicrobial

Table 1 Demographics, patient characteristics, and clinical outcomes among pediatric septic shock latent profile phenotypes in the derivation and validation sets

	Derivation set (n = 646)		p value	Validation set (n = 425)		p value
	Phenotype 1 (n = 126)	Phenotype 2 (n = 520)		Phenotype 1 (n = 71)	Phenotype 2 (n = 354)	
Age (years)	4.7 (1.3, 13.7)	5.4 (1.8, 10.8)	0.698	6.2 (1.8, 14.0)	5.5 (1.8, 10.4)	0.480
Sex (female)	57 (45.2%)	246 (47.3%)	0.676	39 (54.9%)	174 (49.2%)	0.374
Race			0.924			0.439
White or Caucasian	89 (70.7%)	376 (72.3%)		55 (77.4%)	263 (74.3%)	
Black or African American	16 (12.7%)	64 (12.3%)		6 (8.4%)	49 (13.8%)	
Other	21 (16.7%)	80 (15.4%)		10 (14.1%)	42 (11.9%)	
Ethnicity			0.214			0.063
Hispanic or Latino	12 (9.5%)	71 (13.6%)		3 (4.2%)	41 (11.6%)	
Non-Hispanic	114 (90.5%)	449 (86.4%)		68 (95.7%)	313 (88.4%)	
Culture						
Any positive culture	71 (56.4%)	309 (59.4%)	0.529	44 (61.9%)	198 (55.9%)	0.348
Pulmonary	23 (18.2%)	133 (25.6%)		13 (18.3%)	68 (19.2%)	
Extra-pulmonary	48 (38.1%)	175 (33.6%)		31 (43.7%)	130 (36.7%)	
Positive blood culture	33 (26.2%)	100 (19.2%)	0.083	24 (33.8%)	73 (20.6%)	0.016
Pathogen type			0.577			0.467
Gram positive	26 (36.6%)	121 (39.2%)		18 (40.9%)	78 (39.4%)	
Gram negative	28 (39.4%)	122 (39.4%)		17 (38.6%)	88 (44.4%)	
Viral	7 (9.8%)	38 (12.3%)		3 (6.8%)	16 (8.1%)	
Fungal	7 (9.8%)	15 (4.8%)		4 (9.0%)	6 (13.6%)	
Mixed	3 (4.2%)	13 (4.2%)		2 (4.5%)	8 (4.1%)	
Comorbidity						
Heart disease	9 (7.1%)	35 (6.7%)	0.869	4 (5.6%)	24 (6.8%)	0.722
Lung disease	12 (9.5%)	50 (9.6%)	0.975	7 (9.8%)	22 (6.2%)	0.281
Neurologic disease	10 (7.9%)	107 (20.6%)	0.001	9 (12.7%)	67 (18.9%)	0.194
Kidney disease	19 (15.1%)	13 (2.5%)	0.001	5 (7.0%)	10 (2.8%)	0.079
Liver disease	10 (7.9%)	25 (4.8%)	0.164	12 (16.9%)	28 (7.9%)	0.018
Solid organ transplant	5 (4.0%)	13 (2.5%)	0.369	4 (5.6%)	16 (4.5%)	0.686
Oncologic disease	26 (20.6%)	56 (10.8%)	0.003	11 (15.5%)	42 (11.9%)	0.398
Bone marrow transplant	17 (13.5%)	22 (4.3%)	<0.001	9 (12.8%)	29 (8.2%)	0.227
PRISM III	16 (9, 24)	11 (6, 16)	<0.001	16 (11, 23)	10 (6, 15)	<0.001
Day 1 VIS	30 (10, 100)	15 (7, 40)	<0.001	40 (13, 150)	16 (8, 31)	<0.001
Day 1 P/F < 250	31 (24.6%)	118 (22.7%)	0.648	23 (32.4%)	69 (19.5%)	<0.016
PICU LOS	7 (2, 15)	6 (2, 12)	0.673	7 (2, 14)	5 (2, 11)	0.815
PICU Free days	22 (12, 26)	22 (16, 26)	0.668	21 (14, 26)	23 (17, 26)	0.804
Hospital LOS	14 (5, 28)	13 (7, 27)	0.955	15 (3, 28)	14 (7, 26)	0.441
7-day mortality	31 (24.6%)	27 (5.2%)	<0.001	20 (28.2%)	19 (5.4%)	<0.001
28-day mortality	41 (32.5%)	46 (8.9%)	<0.001	25 (35.2%)	30 (8.5%)	<0.001
Complicated course	75 (59.5%)	138 (26.5%)	<0.001	48 (67.6%)	96 (27.1%)	<0.001
Cardiac arrest	67 (53.2%)	76 (14.6%)	<0.001	38 (53.5%)	55 (15.5%)	<0.001
Day 7 Cardiovascular dysfunction	54 (42.8%)	85 (16.4%)	<0.001	36 (50.7%)	71 (20.1%)	<0.001
Day 7 Respiratory Dysfunction	72 (57.2%)	170 (32.7%)	<0.001	46 (64.8%)	120 (33.9%)	<0.001
Day 7 Kidney Dysfunction	64 (50.8%)	104 (20.0%)	<0.001	42 (59.2%)	68 (19.2%)	<0.001
Day 7 Neuro Dysfunction	27 (21.4%)	24 (4.6%)	<0.001	19 (26.8%)	19 (5.4%)	<0.001
Day 7 Hematologic Dysfunction	59 (46.8%)	79 (15.2%)	<0.001	36 (50.7%)	48 (13.6%)	<0.001
Day 7 Hepatic Dysfunction	50 (39.7%)	57 (11.0%)	<0.001	34 (47.9%)	31 (8.8%)	<0.001
Day 7 Vasoactive support [†]	28/70 (40.0%)	55/278 (19.7%)	<0.001	15/39 (38.4%)	40/173 (23.1%)	<0.001

Table 1 (continued)

	Derivation set (n = 646)		p value	Validation set (n = 425)		p value
	Phenotype 1 (n = 126)	Phenotype 2 (n = 520)		Phenotype 1 (n = 71)	Phenotype 2 (n = 354)	
Day 7 Mechanical ventilation [†]	51/70 (72.8%)	164/278 (58.9%)	0.033	30/39 (76.9%)	101/173 (58.3%)	0.031
Day 7 CRRT [†]	27/70 (38.6%)	22/278 (7.9%)	<0.001	10/39 (25.6%)	12/173 (6.9%)	<0.001
Day 1–7% positive fluid balance	6.6 (1.9, 16.6%)	4.9 (0.0, 11.7)	0.016	8.3 (1.7, 17.8)	4.9 (0.7, 11.6)	0.008
Any ECMO	2 (1.6%)	1 (0.2%)	0.039	1 (1.4%)	1 (0.3%)	0.345
Corticosteroids	82 (65.1%)	279 (53.7%)	0.020	53 (74.7%)	187 (52.8%)	<0.001

PRISM III, Pediatric risk of mortality score-III; VIS, vasoactive inotropic score; P/F, PaO₂/FIO₂ ratio; LOS, length of stay; CRRT, Continuous renal replacement therapy; ECMO: Extracorporeal membrane oxygenation. [†]Indicates data only among patients alive and remaining in the PICU on Day 7 after enrollment

Table 2 Logistic regression analyses to test association between latent profile phenotypes across derivation and validation sets and pediatric septic shock outcomes

Variable	Unadjusted OR	Adjusted OR*	p value
Complicated Course			
Phenotype 1 (relative to Phenotype 2)	4.8 (3.5, 6.6)	3.9 (2.8, 5.5)	<0.001
7-day mortality			
Phenotype 1 (relative to Phenotype 2)	6.7 (4.4, 10.2)	5.6 (3.6, 8.6)	<0.001
28-day mortality			
Phenotype 1 (relative to Phenotype 2)	5.6 (3.9, 8.1)	4.4 (3.0, 6.5)	<0.001

*All models adjusted for era of enrollment (2013–2023 vs. 2003–2013), age, PRISM III illness severity score, co-morbidity, and immunocompromised status

Table 3 Unadjusted, inverse probability treatment weighting (IPTW) adjusted association, and overall interaction between latent profile phenotypes and common sepsis treatments on odds of complicated course in the cohort

Treatment effect	Phenotype 1		Phenotype 2		P interaction
	OR (95% CI)	p value	OR (95% CI)	p value	
> 100 ml/kg fluid					
Unadjusted	2.67 (1.47–4.86)	0.0013	1.91 (1.39–2.63)	<0.0001	
IPTW Adjusted	2.93 (1.95–4.38)	<0.0001	1.75 (1.40–2.17)	<0.0001	0.184
≥ 2 Antimicrobials					
Unadjusted	3.53 (1.34–9.31)	0.0108	0.91 (0.55–1.52)	0.7294	
IPTW Adjusted	3.02 (2.00–4.56)	<0.0001	0.82 (0.66–1.01)	0.0577	0.016
≥ 2 Vasoactives					
Unadjusted	2.44 (1.35–4.41)	0.0031	1.91 (1.41–2.59)	<0.0001	
IPTW Adjusted	1.63 (1.07–2.48)	0.0218	1.66 (1.34–2.05)	<0.0001	0.624
Corticosteroids use					
Unadjusted	2.88 (1.55–5.37)	0.0008	1.7 (1.25–2.31)	0.0007	
IPTW Adjusted	2.55 (1.70–3.85)	<0.0001	1.49 (1.20–1.85)	0.0003	0.102

*Inverse probability treatment weighting (IPTW) models adjusted for age, PRISM-III score, vasoactive inotropic score (VIS), co-morbidity, and immunocompromised status

therapies had a higher odds of complicated course in comparison with *Phenotype 2* who had a lower odds of the outcome (interaction *p* value 0.016).

Transcriptomic data was available in 145 patients. We identified 91 differentially expressed genes (DEGs) when comparing patients with *Phenotype 1* (n = 18) versus *Phenotype 2* (n = 127), of which 62 genes were overexpressed

and 29 were underexpressed. The top ten overexpressed genes with an FDR adjusted *p* value <0.05 were *PRTN3*, *ELANE*, *CTSG*, *DEFA3*, *DEFA4*, *CCL4*, *HBB*, *GOS2*, *NEIL3*, and *CEP55*. The top ten under-expressed genes were *SCRT2*, *PRLR*, *ADGRE3*, *FSTL4*, *LGALS1*, *HCAR2*, *RAMP3*, *OLIG2*, *SHE*, and *CMTM2*. Biological pathways enriched among patients with *Phenotype 1* relative

to those *Phenotype 2* corresponded to activation of the immune system, cytokine signaling, neutrophil degranulation, and antimicrobial peptides. CIBERSORT analyses identified that only the proportion of neutrophils was lower among patients with *Phenotype 1* relative to *Phenotype 2*. The volcano plot and results of biological pathway analyses are shown in Fig. 3.

As shown in Fig. 4, the Kwok et al. [26] single-cell RNAseq dataset had 10 cell types from critically ill adult patients with sepsis. Expression data of 58 over-expressed and 19 under-expressed genes identified through DEG analyses distinguishing latent profile phenotypes were available in the single-cell dataset and detailed in the Online Supplement. Genes upregulated among patients with *Phenotype 1* were expressed primarily by a small population of developing neutrophils, and to a lesser extent by CD14 and CD16 positive monocytes, CD4 and CD8 T-cells, natural killer (NK cells), and plasmablasts. Downregulated genes among patients with *Phenotype 1* were expressed primarily by mature neutrophils.

A total of 233 patients in the study had data on established gene-expression endotypes and newly derived latent profile phenotype assignments. There was no statistically significant association between endotypes and phenotypes in the cohort (Pearson χ^2 test, p value of 0.08). Figure 5 shows the Kaplan Meier survival curves based on gene-expression endotype (*Endotype A* vs. *B*),

latent profile phenotype (*Phenotype 1* vs. *Phenotype 2*), and an integrated scheme where we considered all four possible combinations of endotype and phenotype assignment. Patients classified as *Endotype B* & *Phenotype 2* had the lowest mortality risk. Relative to this group, those classified as *Endotype A* & *Phenotype 1* had an over 12-fold (HR 12.5, 95% CI 3.8, 41.2, $p < 0.001$) higher hazard of mortality; those with *Endotype B* & *Phenotype 1* had a nearly fivefold higher hazard of mortality (HR; 4.8, 95% CI 1.1, 20.1, $p = 0.032$); those with *Endotype A* & *Phenotype 2* had an over threefold higher hazard of mortality (HR 3.6, 95% CI 1.2, 11.1, $p = 0.024$). There were no statistically significant differences in mortality between the latter two subclasses.

Discussion

In this study, we derived and internally validated two pediatric septic shock phenotypes, identified through latent profile analyses, of high prognostic relevance. With one exception, there was no evidence for heterogeneous responses to common sepsis treatments on clinical outcomes between phenotypes. Transcriptomic analyses revealed overexpression of genes implicated in innate immune response among those belonging to *Phenotype 1*. Our data suggest a predominance of developing neutrophils among this high-risk subset of patients. We did not identify a statistically significant

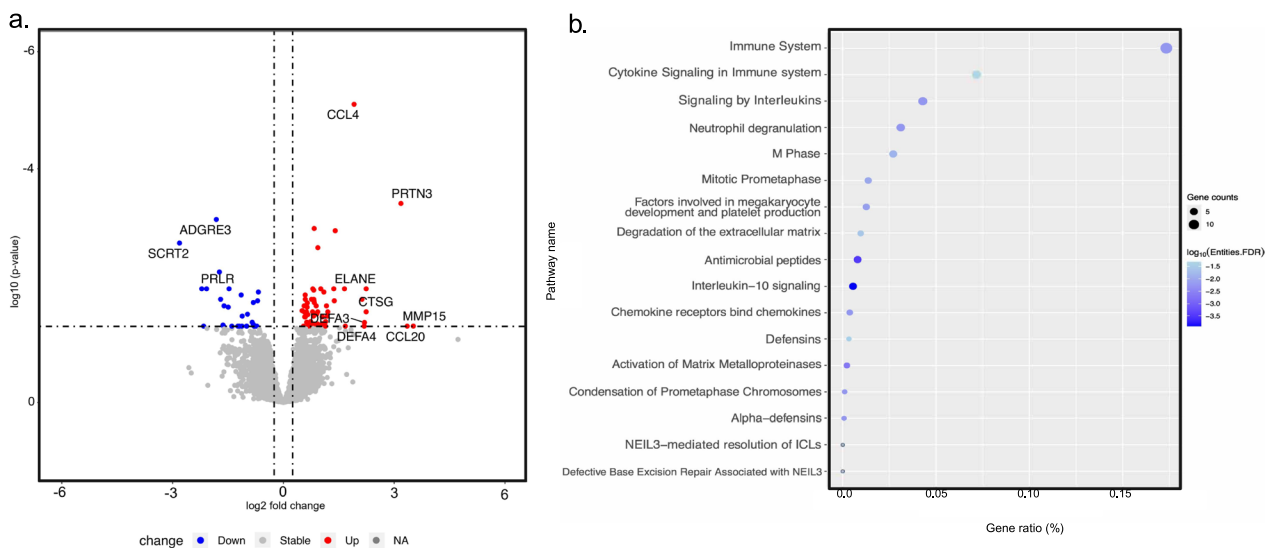


Fig. 3 Transcriptomic assessment of latent profile phenotypes of pediatric septic shock. **a** Volcano plot showing differentially expressed genes among patients belonging to *Phenotype 1* relative to those *Phenotype 2* using a $\log_2(\text{fold change})$ threshold of ± 0.25 . Overexpressed genes are shown in red. Underexpressed genes are shown in blue. The top 10 most differentially expressed genes are labeled including matrix metalloproteinase-15 (*MMP15*), chemokine ligand 20 (*CCL20*), proteinase 3 (*PRTN3*), neutrophil expressed elastase (*ELANE*), cathepsin G (*CTSG*), defensin 3 (*DEFA3*), defensin 4 (*DEFA4*), chemokine ligand 4 (*CCL4*), scratch family transcriptional repressor 2 (*SCRT2*), and adhesion G protein-coupled receptor E3 (*ADGRE3*). **b** Biologically enriched pathways among patients with *Phenotype 1* relative to those in *Phenotype 2*. The y-axis represents the REACTOME pathways enriched for the significantly overexpressed genes. The x-axis represents the gene-ratio (%). The size of the circle indicates gene counts. The darker hue of color indicates a lower adj. p value

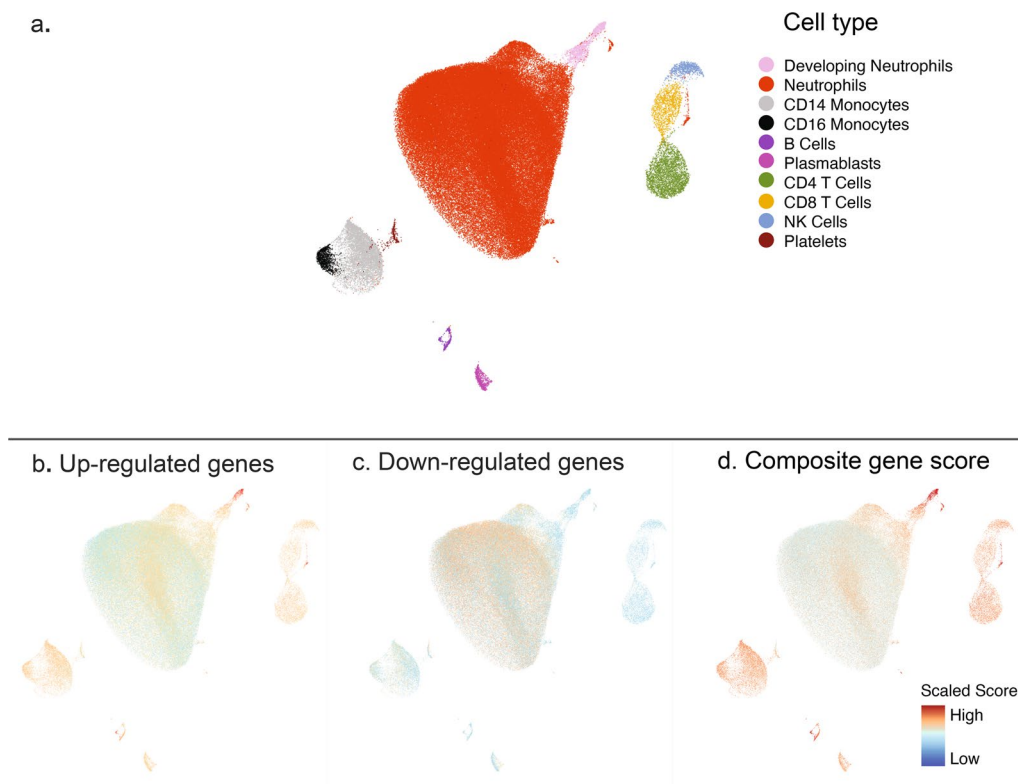


Fig. 4 Inference of cell subsets underlying latent profile phenotypes identified in the study. The figure shows the Uniform Manifold Approximation and Projection (UMAP) of the publicly available single-cell transcriptomic dataset from critically ill adults with sepsis published by *Kwok et al.* **a** Ten cell subsets were identified in the single-cell dataset. (1) Developing neutrophils (pink), (2) Mature neutrophils (red), (3) Cluster differentiation (CD) 14 positive monocytes (light gray), (4) CD16 positive monocytes (black), (5) B lymphocytes (deep purple), (6) PB: Plasmablasts (purple), (7) CD4 positive T lymphocytes (moss green), (8) CD8 positive T lymphocytes (yellow), (9) NK: Natural killer cells (blue), and (10) Platelets (brown). **b** Upregulated genes among patients with *Phenotype 1* shown in red, **c** downregulated genes among patients with *Phenotype 1* shown in blue, and **d** composite gene score representing geometric mean of upregulated minus downregulated genes among patients belonging to *Phenotype 1*. The gene score was scaled as shown in the legend. Cells in red represent those with a high composite gene score indicating that they contributed predominantly to over-expressed genes among patients with *Phenotype 1*. In contrast, cells in blue represent those with a low composite gene score indicating that they contributed predominantly to genes underexpressed among patients with *Phenotype 2*

overlap between established gene-expression endotypes and the newly derived latent profile phenotypes. Finally, we demonstrated the prognostic relevance of patient endophenotypes based on an integrated subclassification scheme that considered both gene-expression-based endotypes and clinico-biomarker latent profile phenotypes.

The phenotypes identified in our study share similarities with the *hyper-* and *hypo-inflammatory* phenotypes originally described by *Calfee* and colleagues among adults with ARDS [13, 14], and subsequently reproduced among other adult [30] and pediatric patients [16]; molecular phenotypes of acute kidney injury detailed by *Bhatraju et al.* among adults [31]; and most recently those identified by *Sinha et al.* among septic adults [18]. Our data provide further support of the reproducibility of latent profile analyses as a methodologic approach to identify phenotypes, irrespective of assigned syndromic

diagnoses, across the spectrum of the host developmental age.

We provide evidence for the prognostic utility of latent profile phenotypes with *Phenotype 1* being independently associated with significant risk of poor clinical outcomes upon adjusting for multiple potential confounders. Unlike previous studies, beyond the robust prognostic implications, we did not find evidence of HTE of common sepsis therapies on clinical outcomes among phenotypes. The exception to this was that those patients with classified as *Phenotype 1* who received ≥ 2 antimicrobial therapies had a significantly higher rate of complicated course than those belonging to *Phenotype 2* who received ≥ 2 antimicrobial therapies. While this observation may merely reflect the fact that *Phenotype 1* represented the sickest subset of patients, a few additional considerations are warranted. *Phenotype 1* may represent patients with an inadequate source control of infection, those with

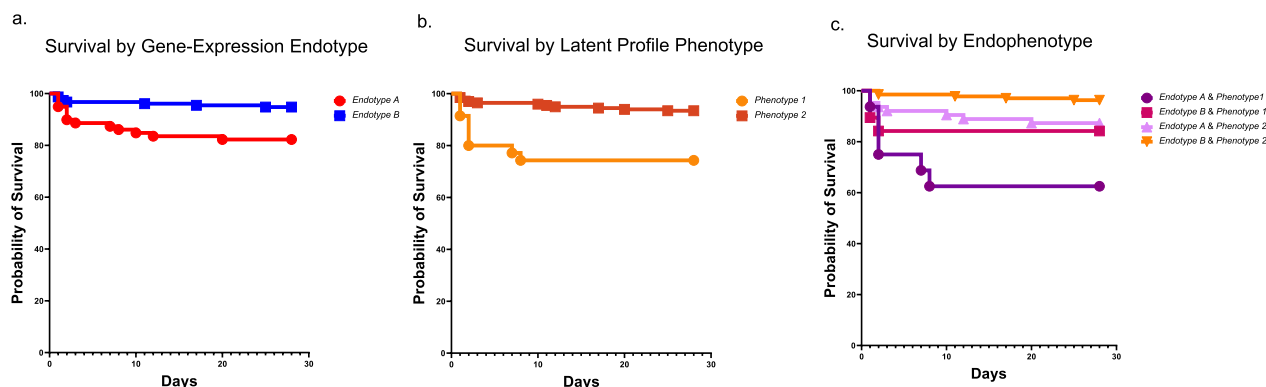


Fig. 5 From left to right, Kaplan Meier survival curves based on **a** established gene-expression endotype (A in red vs. B in blue); Patients with *Endotype A* had a higher hazard of 28-day mortality compared to *Endotype B* (HR 3.7 (95% CI 1.5, 8.7), $p=0.003$), **b** latent profile phenotype (*Phenotype 1* in orange and *Phenotype 2* in brown); Patients with *Phenotype 1* had a higher hazard of 28-day mortality compared to those belonging to *Phenotype 2* (HR 4.5 (95% CI 1.9, 10.6), $p<0.001$). **c** Integrated subclass assignment scheme that considered both the endotype and phenotype assignment among patients including all four possible combinations: (i) *Endotype A/Phenotype 1* (deep purple), (ii) *Endotype B/Phenotype 1* (deep plum), (iii) *Endotype A/Phenotype 2* (light magenta), (iv) *Endotype B/Phenotype 2* (orange). Patients assigned as both *Endotype B* and *Phenotype 2* had the lowest mortality risk. Compared to this group, patients classified as *Endotype A & Phenotype 1* had a higher hazard of mortality (HR 12.5 (95% CI 3.8, 41.2), $p<0.001$). Patients classified as *Endotype B & Phenotype 1* had a hazard ratio of mortality of 4.8 (95% CI 1.1, 20.1, $p=0.032$). Patients classified as *Endotype A & Phenotype 2* had a hazard ratio of mortality of 3.6 (95% CI 1.2, 11.1), $p=0.024$. There were no statistically significant differences between the latter two groups

insufficient therapeutic drug levels of antimicrobials, and patients with an exaggerated host innate immune response, despite appropriate antimicrobial coverage. Of note, our findings mirror those of *Sinha et al.* where the authors identified that septic adults with a *hyperinflammatory* phenotype had higher rates of bacteremia than those without [18]. Pending validation, future studies are needed to determine whether precision antibiotic dosing, targeted use of extra-corporeal blood purification strategies, and or modulation of the innate immune response can be used to improve outcomes among patients with *Phenotype 1*.

We did not identify a differential response to corticosteroids among phenotypes unlike that observed among adults with COVID-19 [15]. The explanations for this difference are likely multifactorial including the relative homogeneity among patients with COVID-19 compared to the cohort studied, differences in pathogen type -viral versus bacterial induced host response, and compartmentalized effects of corticosteroids based on primary cells affected—lung versus peripheral blood. In addition, *Sinha* and colleagues demonstrate differential responses to recombinant activated protein C (rAPC) versus placebo among phenotypes when re-examining results of the PROWESS-SHOCK trial data [18]. While we demonstrate evidence of coagulopathy among those with *Phenotype 1*, we cannot comment on whether latent profile phenotypes among children would be expected to have a similar biological response as with adults, given the developmental differences in host response [32].

Transcriptomic analyses revealed activation of neutrophil pathways consistent with gene-expression studies comparing phenotypes of adult ARDS and sepsis [33–35]. Taken together CIBERSORT analyses and the single-cell composite gene-score data suggest a higher turnover of neutrophils among those with *Phenotype 1* compared to those *Phenotype 2*. These data are intuitive to the clinician and congruent with findings from single-cell multi-omics studies among septic adults, wherein patients with the worst clinical outcomes were characterized by emergency granulopoiesis and the presence of developing neutrophils [26]. Finally, our data suggest a preponderance of additional cell subsets including CD14 and CD16 monocytes, T- and NK-cells, and plasmablasts among *Phenotype 1* patients. While we cannot confidently speak to whether the phenotypes identified represent ‘treatable traits’ [36], our data indicate that the groups identified are biologically distinct. Future studies are necessary to determine the mechanistic link between cell subtypes and phenotypes, and whether targeted modulation of cell subsets can be used as a novel therapeutic approach against sepsis.

We did not identify a statistically significant overlap between established gene-expression-based endotypes and latent profile phenotypes. As such our data suggest that, fundamentally, these two approaches are sampling different, albeit vitally important, biological facets of the host response in critical illness. While the former broadly reflects the adaptive arm of the host immune response, the latter informs the innate arm of the host response,

including microvascular endothelial function. Therefore, we believe that the integrated classification scheme of endophenotypes detailed in our study is of clinical and potential therapeutic relevance. For instance, patients classified as *Endotype A & Phenotype 1* may represent an extreme endophenotype with a significantly increased risk of mortality. This is consistent with the observation that critically ill patients with repressed adaptive- and overactive innate- immune responses have been consistently associated with the worst clinical outcomes [37]. As such these patients would be expected to be poor candidates to receive corticosteroids based on their endotype. However, they may potentially benefit from targeted interventions or immunomodulation to quell the innate immune response based on their phenotypic assignment. Furthermore, although patients with *Endotype B & Phenotype 1* and *Endotype A & Phenotype 2* endophenotypes had comparably elevated risk of mortality, the therapeutic implication of such subclass assignment is expected to be diametrically opposite between groups. Although speculative, pending validation in cohort studies and clinical trials, such an integrated subclassification scheme holds the potential to inform better alignment of interventions among those critically ill by providing a comprehensive understanding of patient-level pathobiology [38].

Our study has several limitations: (1) the observational nature of the study limits precludes inference of causality; (2) despite accounting for era of patient enrollment in our multivariate models, the long study period is a limitation; (3) data missingness especially for biomarker data is a limitation. However, this was mitigated by the use of robust imputation approaches and sensitivity analyses, the latter demonstrating unchanged associations with exclusion of imputed variables in the validation dataset. (4) latent profile phenotypes were based on day 1 data. However, given the temporal and dynamic nature of the host response, it is conceivable that these class assignments may be subject to change over time; (5) external validation dataset to demonstrate the reproducibility of our SVM model was lacking. Moreover, we did not seek to develop a classifier that used a parsimonious set of predictor variables as this is better achieved in external validation sets; (6) given the observational nature of the underlying cohort, interaction effect based upon receipt of ≥ 2 antimicrobials among phenotypes on odds of complicated course is speculative. Although we attempted to address confounding by indication by using IPTW analyses, these data should be interpreted with caution. (7) the number of patients with *Phenotype 1* among whom transcriptomic data was available was limited, which may have contributed to fewer DEGs being identified; (8) the integrated single-cell data used as reference was largely comprised of samples obtained from adults with

sepsis rather than pediatric patients. Further, prospective studies that simultaneously capture phenotypic and single-cell transcriptomic data are necessary to directly identify cell subsets underlying pediatric critical illness subclasses; (9) the number of patients in whom both established gene-expression endotype and latent profile phenotype class assignments were available was limited; (10) both endotype and phenotype assignments were based on data generated within 24 h of meeting septic shock criteria and were assumed to reflect baseline differences in host response. However, a significant proportion of patients in the cohort received corticosteroids. It remains plausible that the biological differences in host response among subclasses may reflect those in response to corticosteroids, rather than baseline differences.

Conclusions

In this study, we demonstrate the existence of two phenotypes among children with septic shock identified through latent profile analyses with high prognostic value. We provide evidence of upregulated host innate responses including microvascular endothelial dysfunction among those with *Phenotype 1* with transcriptomic evidence of high turnover of neutrophils. The phenotypes did not show overlap with established gene-expression-based endotypes in pediatric septic shock nor demonstrate a differential response to corticosteroids. We integrated these two promising classification schemes to delineate novel sepsis ‘endophenotypes.’ Pending validation, such an approach may allow for therapeutic drug selection informed by a comprehensive understanding of patient-level pathobiology.

Supplementary Information

The online version contains supplementary material available at <https://doi.org/10.1186/s13054-024-05020-z>.

Additional file 1.

Acknowledgements

The authors are indebted to the contributions of Dr. Hector Wong (H.R.W.). H.R.W.’s NIH R35GM126943 award partially funded this work. Kelli Harmon and Patrick Lahni maintained the biobank and conducted experiments, respectively. Drs. Geoffrey Allen (Children’s Mercy Hospital, Kansas City, MO) and Jocelyn Grunwell (Children’s Healthcare of Atlanta at Egleston, Atlanta, GA) contributed to patient recruitment but did not contribute to the manuscript. Transcriptomic data were made available through the SUBSPACE (Subtyping in Sepsis and Critical Illness) Consortium, funded, and managed by Inflammatrix, Inc.

Author contributions

Study conceptualization: M.R.A. and R.K. Funding acquisition: M.R.A., N.S.P., and R.K. Data acquisition: M.R.A., J.C.F., N.Z.C., S.L.W., M.T.B., P.N.J., A.J.S., R.L. J.N., N.J.T., M.Q., B.H., T.B., P.K., and T.E.S.; Project administration: A.J.L., N.L.S., S.W.S., J.M.K., and B.Z. Data curation and analyses: M.R.A., M.H., A.R.M., H.Z., Y.H.B., R.S., B.Z., P.K. and R.K. Draft of the manuscript: M.R.A., M.H., A.R.M. Critical review for important

intellectual content and interpretation of data: M.K.D and P.K. All authors approve the manuscript in its final version.

Funding

M.R.A was supported by the Cincinnati Children's Research Foundation through a Procter K-to-R Scholar award and by the National Institute of General Medical Sciences (NIGMS) of the National Institutes of Health (NIH) under award number R35GM155165. M.R.A, N.S.P, and R.K received funding through NIH award R21GM151703 for this work. M.R.A and A.J.L were supported by R21GM150093. N.S.P received funding through R21GM146159 and R01HD105939. M.D received funding through R01HL149910. R.K received funding through R21GM148931 and R01GM139967.

Data availability

All de-identified clinical data and bulk messenger RNA sequencing (fastq) files and related metadata are available upon reasonable request to the corresponding author.

Declarations

Ethical approval and consent to participate

The study protocol was approved by Institutional Review Boards (IRBs) of the primary site (Cincinnati Children's Hospital IR, Genomic Analysis of Pediatric Systemic Inflammatory Syndrome, IRB ID: 2008-0558) as well as all participating institutions. Informed consent was obtained from parent or guardian of patients. All procedures performed in studies involving human participants were in accordance with the ethical standards of the institutional review boards of participating institutions and with the 1964 Helsinki declaration and its later amendments or comparable ethical standards.

Competing interests

Cincinnati Children's Hospital Medical Center (CCHMC) and the estate of the late Dr. Hector R. Wong hold patents for gene-expression-based pediatric septic shock endotypes, reflective of the host adaptive immune system. M.R.A and R.K hold a provisional patent for gene-expression-based multiple organ dysfunction syndrome (MODS) subclass identification, reflective of the host innate immune response. Inflammix is a for-profit company focused on the development and commercialization of best-in-class host-response diagnostic tests. Y.H.B and T.E.S are employees and/or stockholders of Inflammix Inc. P.K is a stockholder of Inflammix Inc.

Author details

¹Division of Critical Care Medicine, MLC2005, Cincinnati Children's Hospital Medical Center, 3333 Burnet Avenue, Cincinnati, OH 45229, USA. ²Department of Pediatrics, University of Cincinnati College of Medicine, Cincinnati, OH 45627, USA. ³Department of Biomedical Informatics, Emory University School of Medicine, Atlanta, GA, USA. ⁴Stanford Institute for Immunity, Transplantation and Infection, Stanford University School of Medicine, Stanford, CA, USA. ⁵Center for Biomedical Informatics Research, Department of Medicine, Stanford University School of Medicine, Stanford, CA 94305, USA. ⁶Inflammix, Sunnyvale, CA 94085, USA. ⁷Children's Hospital of Philadelphia, Philadelphia, PA 19104, USA. ⁸Nemours Children's Health, Wilmington, DE 19803, USA. ⁹UCSF Benioff Children's Hospital Oakland, Oakland, CA 94609, USA. ¹⁰Akron Children's Hospital, Akron, OH 44308, USA. ¹¹Texas Children's Hospital, Baylor College of Medicine, Houston, TX 77030, USA. ¹²Children's Hospital of Orange County, Orange, CA 92868, USA. ¹³Riley Hospital for Children, Indianapolis, IN 46202, USA. ¹⁴Children's Hospital and Clinics of Minnesota, Minneapolis, MN 55404, USA. ¹⁵Penn State Hershey Children's Hospital, Hershey, PA 17033, USA. ¹⁶C.S Mott Children's Hospital, University of Michigan, Ann Arbor, MI 48109, USA. ¹⁷University of Florida Health Children's Hospital, Gainesville, FL 32610, USA. ¹⁸Lucile Packard Children's Hospital Stanford, Palo Alto, CA 94304, USA. ¹⁹Division of Biostatistics and Epidemiology, Cincinnati Children's Hospital Medical Center, Cincinnati, OH 45229, USA. ²⁰Department of Pediatrics, Northwestern University Feinberg School of Medicine, Chicago, IL 60611, USA. ²¹Department of Health and Biomedical Informatics, Northwestern University Feinberg School of Medicine, Chicago, IL 60611, USA. ²²Department of Biomedical Informatics, Emory University School of Medicine, Atlanta, GA 30322, USA. ²³Department of Biomedical Engineering, Georgia Institute of Technology, Atlanta, GA 30322, USA.

Received: 10 March 2024 Accepted: 5 July 2024

Published online: 17 July 2024

References

- Rudd KE, Johnson SC, Agesa KM, Shackelford KA, Tsoi D, Kievlan DR, et al. Global, regional, and national sepsis incidence and mortality, 1990–2017: analysis for the Global Burden of Disease Study. *Lancet*. 2020;395(10219):200–11.
- Global report on the epidemiology and burden of sepsis: current evidence, identifying gaps and future directions. World Health Organization. 2020. p.56. Available from: <https://apps.who.int/iris/bitstream/handle/10665/334216/9789240010789-eng.pdf?sequence=1&isAllowed=y>
- Marshall JC. Why have clinical trials in sepsis failed? *Trends Mol Med*. 2014;20(4):195–203.
- Shah FA, Meyer NJ, Angus DC, Awdish R, Azoulay É, Calfee CS, et al. A research agenda for precision medicine in sepsis and acute respiratory distress syndrome: an Official American Thoracic Society Research Statement. *Am J Respir Crit Care Med*. 2021;204(8):891–901.
- Wong HR, Cvijanovich N, Lin R, Allen GL, Thomas NJ, Willson DF, et al. Identification of pediatric septic shock subclasses based on genome-wide expression profiling. *BMC Med*. 2009;7:34.
- Davenport EE, Burnham KL, Radhakrishnan J, Humburg P, Hutton P, Mills TC, et al. Genomic landscape of the individual host response and outcomes in sepsis: a prospective cohort study. *Lancet Respir Med*. 2016;4(4):259–71.
- Scicluna BP, van Vught LA, Zwinderman AH, Wiewel MA, Davenport EE, Burnham KL, et al. Classification of patients with sepsis according to blood genomic endotype: a prospective cohort study. *Lancet Respir Med*. 2017;5(10):816–26.
- Sweeney TE, Perumal TM, Henao R, Nichols M, Howrylak JA, Choi AM, et al. A community approach to mortality prediction in sepsis via gene expression analysis. *Nat Commun*. 2018;9(1):694.
- Yang JO, Zinter MS, Pellegrini M, Wong MY, Gala K, Markovic D, et al. Whole blood transcriptomics identifies subclasses of pediatric septic shock. *Crit Care*. 2023;27(1):486.
- Wong HR, Cvijanovich N, Lin R, Allen GL, Thomas NJ, Willson DF, et al. Identification of pediatric septic shock subclasses based on genome-wide expression profiling. *BMC Med*. 2009;7(1):34.
- Wong HR, Cvijanovich NZ, Anas N, Allen GL, Thomas NJ, Bigham MT, et al. Developing a clinically feasible personalized medicine approach to pediatric septic shock. *Am J Respir Crit Care Med*. 2015;191(3):309–15.
- Antcliffe DB, Burnham KL, Al-Beidh F, Santhakumaran S, Brett SJ, Hinds CJ, et al. Transcriptomic signatures in sepsis and a differential response to steroids. From the VANISH randomized trial. *Am J Respir Crit Care Med*. 2019;199(8):980–6.
- Calfee CS, Delucchi K, Parsons PE, Thompson BT, Ware LB, Matthay MA, et al. Subphenotypes in acute respiratory distress syndrome: latent class analysis of data from two randomised controlled trials. *Lancet Respir Med*. 2014;2(8):611–20.
- Calfee CS, Delucchi KL, Sinha P, Matthay MA, Hackett J, Shankar-Hari M, et al. ARDS subphenotypes and differential response to simvastatin: secondary analysis of a randomized controlled trial. *Lancet Respir Med*. 2018;6(9):691–8.
- Sinha P, Furfaro D, Cummings MJ, Abrams D, Delucchi K, Maddali MV, et al. Latent class analysis reveals COVID-19-related acute respiratory distress syndrome subgroups with differential responses to corticosteroids. *Am J Respir Crit Care Med*. 2021;204(11):1274–85.
- Dahmer MK, Yang G, Zhang M, Quasney MW, Sapru A, Weeks HM, et al. Identification of phenotypes in paediatric patients with acute respiratory distress syndrome: a latent class analysis. *Lancet Respir Med*. 2022;10(3):289–97.
- Yehya N, Zinter MS, Thompson JM, Lim MJ, Hanudel MR, Alkhouli MF, et al. Identification of molecular subphenotypes in two cohorts of paediatric ARDS. *Thorax*. 2023;thorax-2023–220130.
- Sinha P, Kerchberger VE, Willmore A, Chambers J, Zhuo H, Abbott J, et al. Identifying molecular phenotypes in sepsis: an analysis of two prospective observational cohorts and secondary analysis of two randomised controlled trials. *Lancet Respir Med*. 2023

19. Wong HR, Caldwell JT, Cvijanovich NZ, Weiss SL, Fitzgerald JC, Bigham MT, et al. Prospective clinical testing and experimental validation of the Pediatric Sepsis Biomarker Risk Model. *Sci Transl Med.* 2019;11:518.
20. Atreya MR, Cvijanovich NZ, Fitzgerald JC, Weiss SL, Bigham MT, Jain PN, et al. Integrated PERSEVERE and endothelial biomarker risk model predicts death and persistent MODS in pediatric septic shock: a secondary analysis of a prospective observational study. *Crit Care.* 2022;26(1):210.
21. Atreya MR, Cvijanovich NZ, Fitzgerald JC, Weiss SL, Bigham MT, Jain PN, et al. Prognostic and predictive value of endothelial dysfunction biomarkers in sepsis-associated acute kidney injury: risk-stratified analysis from a prospective observational cohort of pediatric septic shock. *Crit Care.* 2023;27(1):260.
22. Goldstein B, Giroir B, Randolph A, International Consensus Conference on Pediatric Sepsis. International pediatric sepsis consensus conference: definitions for sepsis and organ dysfunction in pediatrics. *Pediatr Crit Care Med.* 2005;6(1):2–8.
23. Bießmann F, Rukat T, Schmidt P, Naidu P, Schelter S, Taptunov A, et al. DataWig: Missing value imputation for tables.
24. Wong HR, Cvijanovich NZ, Anas N, Allen GL, Thomas NJ, Bigham MT, et al. PERSEVERE-II: Redefining the pediatric sepsis biomarker risk model with septic shock phenotype. *Crit Care Med.* 2016;44(11):2010–7.
25. Fabregat A, Jupe S, Matthews L, Sidiropoulos K, Gillespie M, Garapati P, et al. The reactome pathway knowledgebase. *Nucleic Acids Res.* 2018;46(D1):D649–55.
26. Kwok AJ, Allcock A, Ferreira RC, Cano-Gamez E, Smee M, Burnham KL, et al. Neutrophils and emergency granulopoiesis drive immune suppression and an extreme response endotype during sepsis. *Nat Immunol.* 2023;24(5):767–79.
27. Zheng H, Rao AM, Dermadi D, Toh J, Murphy Jones L, Donato M, et al. Multi-cohort analysis of host immune response identifies conserved protective and detrimental modules associated with severity across viruses. *Immunity.* 2021;54(4):753–768.e5.
28. Pollack MM, Patel KM, Ruttimann UE. The Pediatric Risk of Mortality III–Acute Physiology Score (PRISM III-APS): a method of assessing physiologic instability for pediatric intensive care unit patients. *J Pediatr.* 1997;131(4):575–81.
29. Chesnaye NC, Stel VS, Tripepi G, Dekker FW, Fu EL, Zoccali C, et al. An introduction to inverse probability of treatment weighting in observational research. *Clin Kidney J.* 2021;15(1):14–20.
30. Bos LD, Schouten LR, van Vught LA, Wiewel MA, Ong DSY, Cremer O, et al. Identification and validation of distinct biological phenotypes in patients with acute respiratory distress syndrome by cluster analysis. *Thorax.* 2017;72(10):876–83.
31. Bhatraju PK, Zelnick LR, Herting J, Katz R, Mikacenic C, Kosamo S, et al. Identification of acute kidney injury subphenotypes with differing molecular signatures and responses to vasopressin therapy. *Am J Respir Crit Care Med.* 2019;199(7):863–72.
32. Nadel S, Goldstein B, Williams MD, Dalton H, Peters M, Macias WL, et al. Drotrecogin alfa (activated) in children with severe sepsis: a multicentre phase III randomised controlled trial. *Lancet.* 2007;369(9564):836–43.
33. Bos LDJ, Scicluna BP, Ong DSY, Cremer O, van der Poll T, Schultz MJ. Understanding heterogeneity in biologic phenotypes of acute respiratory distress syndrome by leukocyte expression profiles. *Am J Respir Crit Care Med.* 2019;200(1):42–50.
34. Neyton LPA, Sinha P, Sarma A, Mick E, Kalantar K, Chen S, et al. Host and microbe blood metagenomics reveals key pathways characterizing critical illness phenotypes. *Am J Respir Crit Care Med.* 2024
35. Sinha P, Neyton L, Sarma A, Wu N, Jones C, Zhuo H, et al. Molecular phenotypes of ARDS in the ROSE trial have differential outcomes and gene expression patterns that differ at baseline and longitudinally over time. *Am J Respir Crit Care Med.* 2024
36. de Grooth HJ, Cremer OL. Beyond patterns: how to assign biological meaning to ARDS and sepsis phenotypes. *Lancet Respir Med.* 2023
37. Sweeney TE, Azad TD, Donato M, Haynes WA, Perumal TM, Henao R, et al. Unsupervised analysis of transcriptomics in bacterial sepsis across multiple datasets reveals three robust clusters. *Crit Care Med.* 2018;46(6):915–25.
38. van Amstel RBE, Kennedy JN, Scicluna BP, Bos LDJ, Peters-Sengers H, Butler JM, et al. Uncovering heterogeneity in sepsis: a comparative analysis of subphenotypes. *Intensive Care Med.* 2023. <https://doi.org/10.1007/s00134-023-07239-w>.

Publisher's Note

Springer Nature remains neutral with regard to jurisdictional claims in published maps and institutional affiliations.